COMPUTATIONAL AEROACOUSTIC ANALYSIS OF INDUSTRIAL FAN APPLICATION USING A HYBRID APPROACH

Marie CABROL[1], Yves DETANDT[1], Fred MENDONCA[2], Diego d'UDEKEM[1], Julien MANERA[1]

[1] *Free Field Technologies, Axis Park, rue E. Francqui, 1435 Mont-Saint-Guibert, Belgium*

[2] *CD-Adapco, 200 Sheperds Bush Road, W6 7NL, London, United Kingdom*

SUMMARY

This paper presents a hybrid aeroacoustic method in the finite element context. The approach decomposes the aerodynamic noise sources in a boundary and a volume contribution. The importance of these contributions is analyzed on a simplified centrifugal fan. The example involves the vibrations induced on the casing of the system and generating noise outside the system.

INTRODUCTION

Many industrial applications involve a fan component in the system. This part of the system is generally the main contribution to the noise generated by the system: this justifies to focus on this component in order to estimate which design decreases the perceived noise outside the HVAC system. The industrial requirements involve not only a global sound level, but a maximum noise level for each frequency range. The new designs are compared thanks to different computational validation tools. In the present paper, we illustrate a Finite Element Method based on Lighthill analogy. The noise inside the acoustic fluid generated by the rotating part is transmitted through the casing and communicated to the exterior of the system. Even if the method is demonstrated on a simplified problem, it shows how it provides a useful understanding of the noise generation and propagation mechanisms in the system (from the acoustic fluid inside the system to the exterior). Based on the noise sources related to a given setup, different materials could be applied on the casing in order to reduce the noise level.

In the first part of the paper, we detail briefly the theoretical background of the acoustic model.

In the second part of the paper, we illustrate the concept on a simplified centrifugal fan system which is representative of an industrial configuration. Indeed an industrial configuration will not need additional modeling means. The main difference between an industrial model and the model

studied in this paper concerns the CFD mesh refinement which could me more important on an industrial problem.

NUMERICAL METHOD

Finite element aeroacoustic formulation

The modeling is based on a variational statement based on the Lighthill equation. The Lighthill equation is derived by rearranging the continuity and momentum equations:

$$\frac{\partial^2 \tilde{\rho}}{\partial t^2} - \frac{\partial}{\partial x_i}\left(c_0^2 \frac{\partial \tilde{\rho}}{\partial x_i} \right) = \frac{\partial^2 \tilde{T}_{ij}}{\partial x_i \partial x_j}$$

The density in the left hand side corresponds to the acoustic solution in the far field. The right hand side is computed using the unsteady solution provided by the CFD simulation. This equation could be solved in the time domain, but the acoustic treatments are easily modeled in the frequency domain. Performing a Fourier transform leads to an equivalent equation in the frequency domain:

$$\tilde{q}(\vec{x},t) = \sum_{\omega} q(\vec{x}) e^{i\omega t}$$

$$-\omega^2 \rho - \frac{\partial}{\partial x_i}\left(c_0^2 \frac{\partial \rho}{\partial x_i} \right) = \frac{\partial^2 T_{ij}}{\partial x_i \partial x_j}$$

This equation is multiplied by a Galerkin weight function which is related to the acoustic mesh. Integrating over the acoustic domain leads to the variational form:

$$\omega^2 \int_V N_a \rho dV - \int_V \frac{\partial N_a}{\partial x_i} c_0^2 \frac{\partial \rho}{\partial x_i} dV = i\omega \oint_S N_a \rho v_i n_i dS + \int_V \frac{\partial N_a}{\partial x_i} \frac{\partial T_{ij}}{\partial x_j} dV$$

Some terms have been integrated by parts and rearranged thanks to the Green theorem. These mathematical operations are perfectly licit and not introducing any additional hypothesis. This formulation is therefore as general as the rearrangement of Navier-Stokes equations leading to the Lighthill equation. The polynomial order of the weight function directly influences the performance of the acoustic numerical scheme (number of elements per acoustic wavelength). The performances of the scheme are sometimes tuned thanks to some super-convergence properties of dedicated elements.

The left hand side corresponds to the acoustic wave propagation operator. This operator correctly mimics the wave propagation in a medium animated by a low speed mean flow. For higher Mach number based on the mean flow velocity, more complex operators are preferred. These more complex operators are present in Actran, but the present test Mach number did not justify the use of a complex wave propagation operator.

The right hand side corresponds to two equivalent aeroacoustic sources. The first one is computed over a surface and corresponds to distributed forces acting on the acoustic fluid. The second one is a volume force distributed over the acoustic source domain and corresponding to the noise associated to the turbulent fluctuations. The surface contribution may represent many physical excitations:

- Vibrations induced by an external system acting on the acoustic fluid
- Fluctuations coming from an external acoustic domain.

As the rotating part is not part of the acoustic model, the surface contribution is used to record the acoustic fluctuations flowing from the rotor to the static part of the domain. This contribution and the volume sources are computed from the unsteady flow field.

Finite element vibroacoustic formulation

The previous section described the acoustic wave generation and propagation mechanism in the acoustic fluid. The acoustic pressure wave hits the fan casing and the panels of the system surrounding the downstream components of the fan (HVAC system). The acoustic pressure fluctuations emanating from the acoustic fluid generates an unsteady force acting on the structural components of the system. The structure loaded by this unsteady force due to acoustic field follows the elasticity equations, which relates the displacement to the pressure forces acting on the solid surface. Different levels of approximation are available (elastic solid, thin shell, visco-elastic material, …) to model the casing of the system. On the interface between the structure and the acoustic fluid, the two set of equations are coupled thanks to the boundary contributions: the pressure forces generated on the acoustic fluid acts on the structure surface which in turns produces a normal velocity contribution acting on the fluid. This strong coupling ensures the conversion of the acoustic pressure fluctuations in structural waves which radiates acoustic fluctuations outside the system.

Computational process

The computational process illustrated in Figure 1 is decomposed into two separate and distinct tasks performed by different teams. STAR-CCM+ provides an unsteady turbulent flow at all the time steps. The CFD simulation could be optimized thanks to the wide range of available turbulence models, schemes and meshing tools, which cover most potential applications. In a second step, the unsteady flow velocity and density fields are processed in Actran to generate equivalent acoustic sources. The acoustic pre-processing involves reading the native STAR-CCM+ mesh and solution format, computing the acoustic sources, and projecting these results onto an acoustic grid, which is designed for an accurate acoustic propagation. The flow and the acoustics are decoupled.

The flow is generally not sensitive to the small acoustic fluctuations. A single CFD results can therefore be used to assess or design the acoustic treatment applied close to identified flow noise sources.

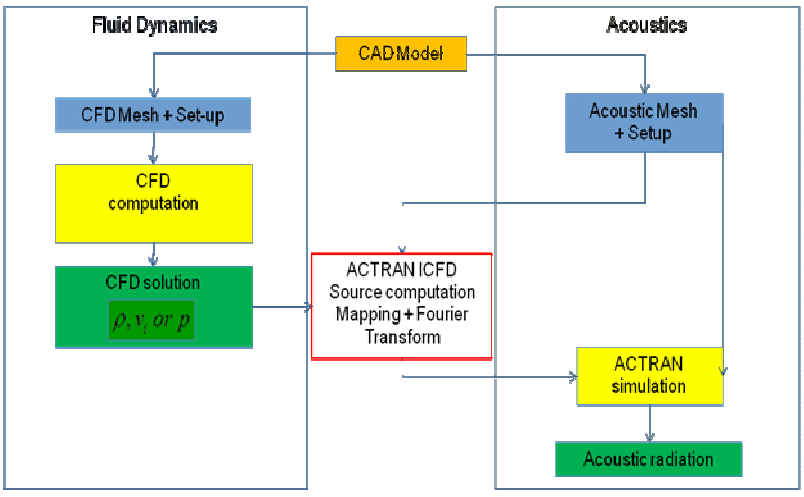

Figure 1: Computational process overview for aeroacoustic simulation with Actran

NUMERICAL MODELING

Problem statement

This work consists in studying the noise generated by a radial fan made of twelve blades and illustrated in Figure 2.

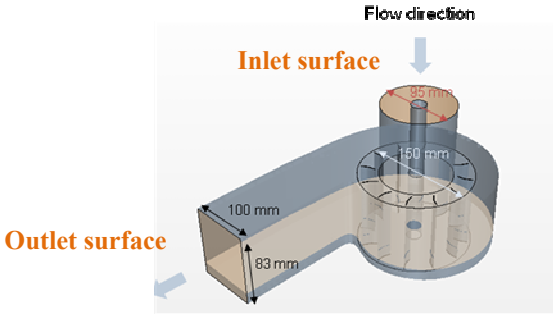

Figure 2: Fan geometry

The fan noise comes from the unsteady aerodynamic phenomenon generated around the blades in rotation. For such a configuration, a tonal noise is expected at particular frequencies named the Blade Passing Frequencies (BPF). In our application, based on a 2000 rpm rotating speed of the twelve blades fan, the blade passing frequency is 400Hz.

$$BPF = \frac{Nt}{60}$$

With:

- N: Rotating speed
- t: Number of blades

Numerical setup for aeroacoustic analysis

The acoustic domain involves at least the CFD domain which corresponds to the source region. Only the static part is modeled with a volume mesh, the rotating being not part of the acoustic model. The interface between static and rotating part is devoted to receive the surface contribution as explained in the theoretical section. The mesh is made of quadratic tetrahedral elements whose maximal length allows performing an acoustic analysis up to 2000 Hz.

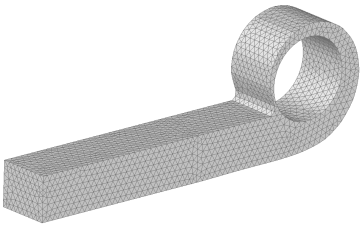

Figure 3: Acoustic mesh

The finite fluid domain is made of two volume domains as illustrated in Figure 4:

- The *CAA* domain: same than the CFD outlet static domain;
- The *Buffer* domain: outlet duct extension where no sources are computed; At the end of this region, a non reflective boundary condition is applied (i.e. anechoic termination).

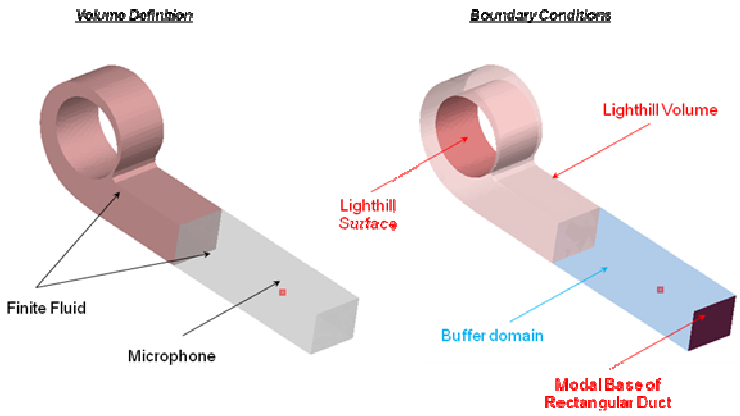

Figure 4: Aeroacoustic model

A virtual microphone is placed in the duct downstream the fan to record the acoustic solution. The following boundary conditions are applied:

- A volume contribution applied on the acoustic domain where the volume sources are computed from the unsteady CFD results;
- A surface contribution applied on the interface between the CFD rotating and static domains; on this surface, the sources located in the CFD rotating domain are computed.

Different loadcases are defined in the analysis in order to study the contribution of the two Lighthill boundary conditions in the total noise generated by the fan. One loadcase contains only the contribution of the CAA sources applied on the interface between static and rotating parts while the second loadcase only contains the contribution of the CAA sources applied on the volume. A third loadcase including both boundary conditions is also available (the results being the sum of the two previous loadcases).

Numerical setup for aero-vibro-acoustic analysis

The aero-vibro-acoustic model corresponds to a fan flowing air in a flexible finite length duct, finally leading air into the anechoic room. The fan and duct casing are made of different materials to investigate the effects of the vibrations on near and far field acoustics. The different configurations are summarized in Table 1. The rigid configuration will be the baseline configuration for comparisons.

Table 1: Characteristics of aero-vibro-acoustic models

Configuration	E (GPa)	Density (kg/m^3)	Poisson ratio	Damping
Rigid	∞	0	0	0
Steel	210	7850	0.3	0.1%
Aluminum	70	2700	0.3	0.1%

The model is presented in Figure 5. The mesh on the structure is designed to correctly capture the bending wavelength for all the configurations up to 2kHz. The mesh for the interior domain inside the duct corresponds to the one presented in the aeroacoustic setup. A similar mesh criterion has been used for the exterior domain mesh, leading to a setup valid up to 2kHz. The meshes between the interior and exterior domains are not conformal. The interface between these two meshes

insures continuity of the acoustic pressure between the interior and exterior degrees of freedom. In all configurations, the mesh is identical, only material parameters for the casing have been changed. The infinite elements surround the finite element domain and impose the non-reflecting boundary condition.

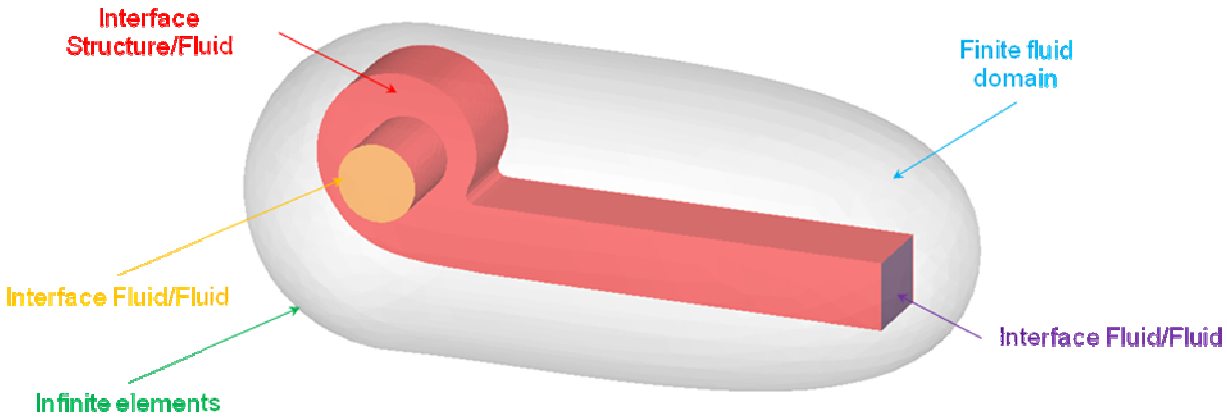

Figure 5: Aero-vibro-acoustic model

The Table 2 compares the computational requirements of the aeroacoustic and aero-vibro-acoustic setups.

Table 2: Computational requirements

Configuration	RAM memory	Computational time /frequency/CPU
Aeroacoustic	2 GB	45 s
Aero-vibro-acoustic	4.8 GB	4 min 8 s

RESULTS

Aeroacoustic analysis

The Figure 6 provides the Sound Pressure Level (SPL) at the inner virtual microphone (field point) for the different loadcases. The aeroacoustic calculations are based on a compressible CFD simulation. The SPL shows a tonal behavior as expected with the emergence of the BPF and its harmonics.

The total noise at the microphone is clearly driven by the contribution of the Lighthill surface boundary condition, representing the sources located in the rotating area. As expected, it means that most of the aero-acoustics sources are located close to the blades.

The same conclusion can be drawn by analyzing the acoustic incident power transmitted on the outlet section (Figure 7).

Aero-vibro-acoustic analysis

In the aero-vibro-acoustic model, the duct induces a set of acoustic duct modes which are presented in Figure 8. These modes are longitudinal resonant modes, section transverse modes being cutoff in

the present setup below 1700 Hz. These are not related to the vibration of the structure and will add additional peaks in the SPL at these resonant frequencies (Figure 9).

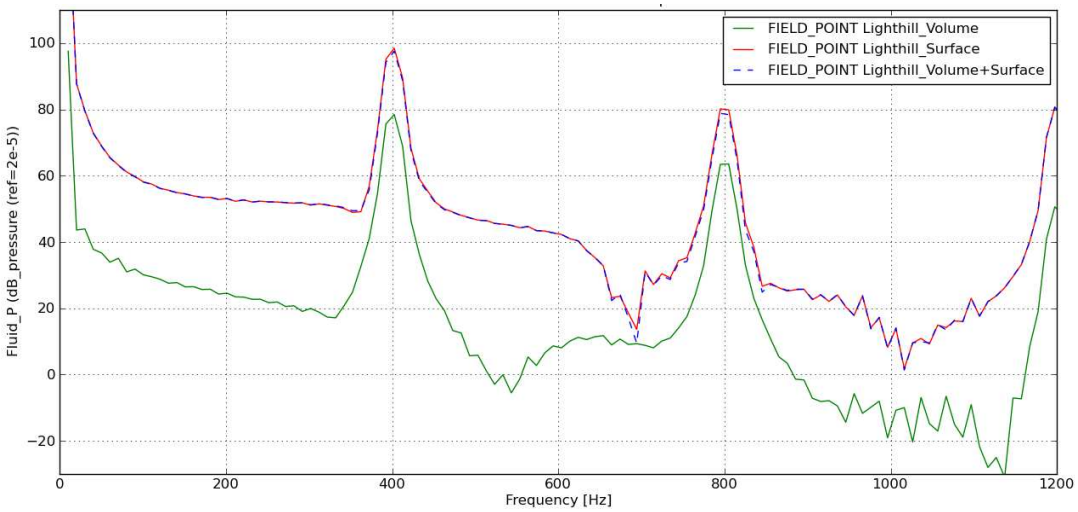

Figure 6: SPL at the virtual microphones - Contribution of the boundary conditions

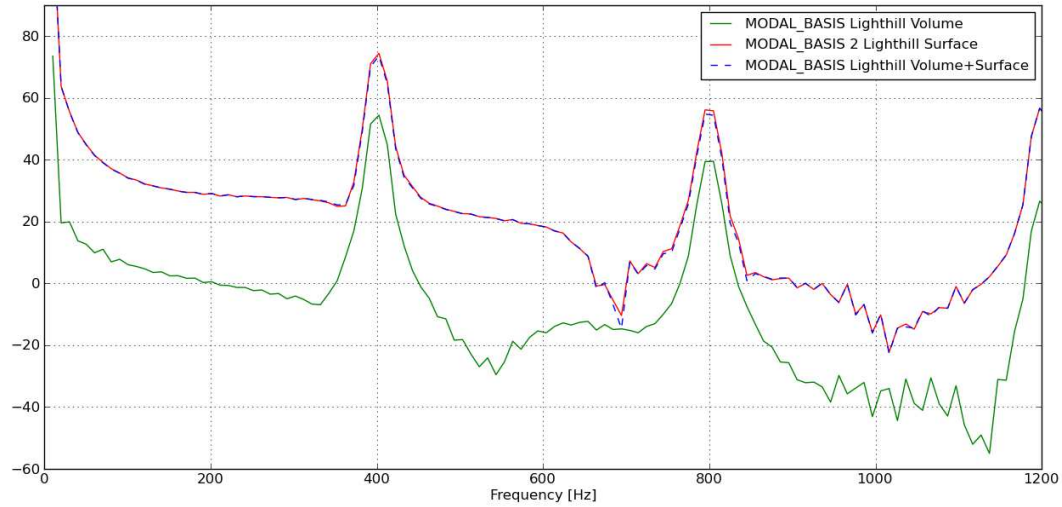

Figure 7: Acoustic power transmitted on the outlet section - Contribution of the boundary conditions

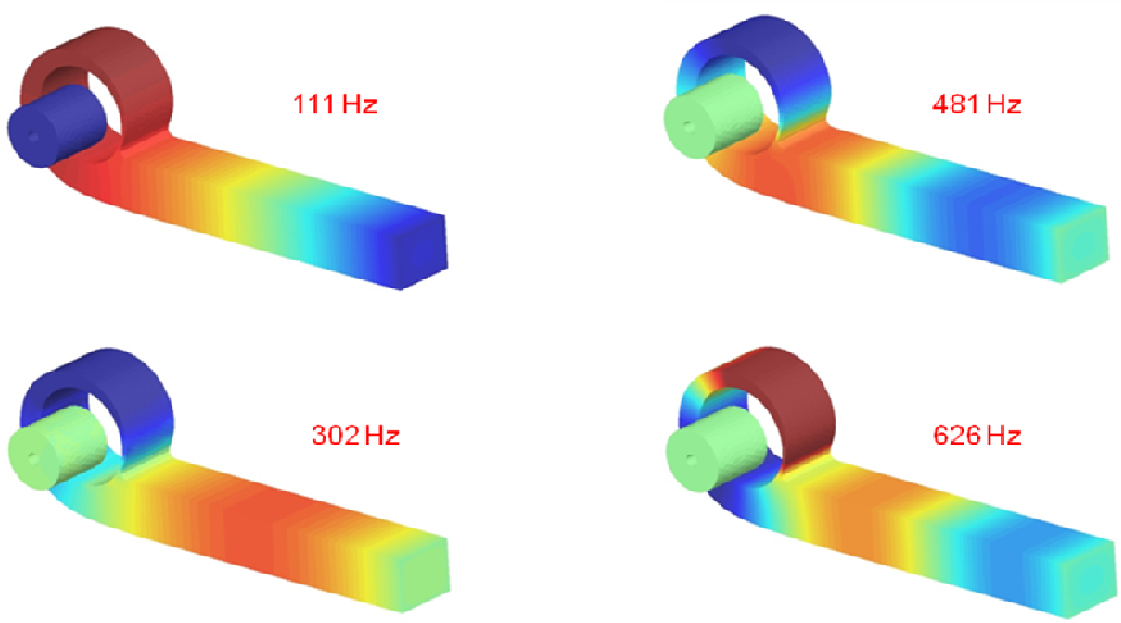

Figure 8: Acoustic duct modes

The peaks observed at 400, 800 and 1200 Hz correspond to the blade passing frequencies which are the mode of the aeroacoustic excitation as explained in the previous section. The peaks observed at 111, 302, 481 and 626 Hz are due to acoustic resonances of the duct. Shorter or longer duct or different cross section dimensions will change the values of these frequencies and the associated mode shapes.

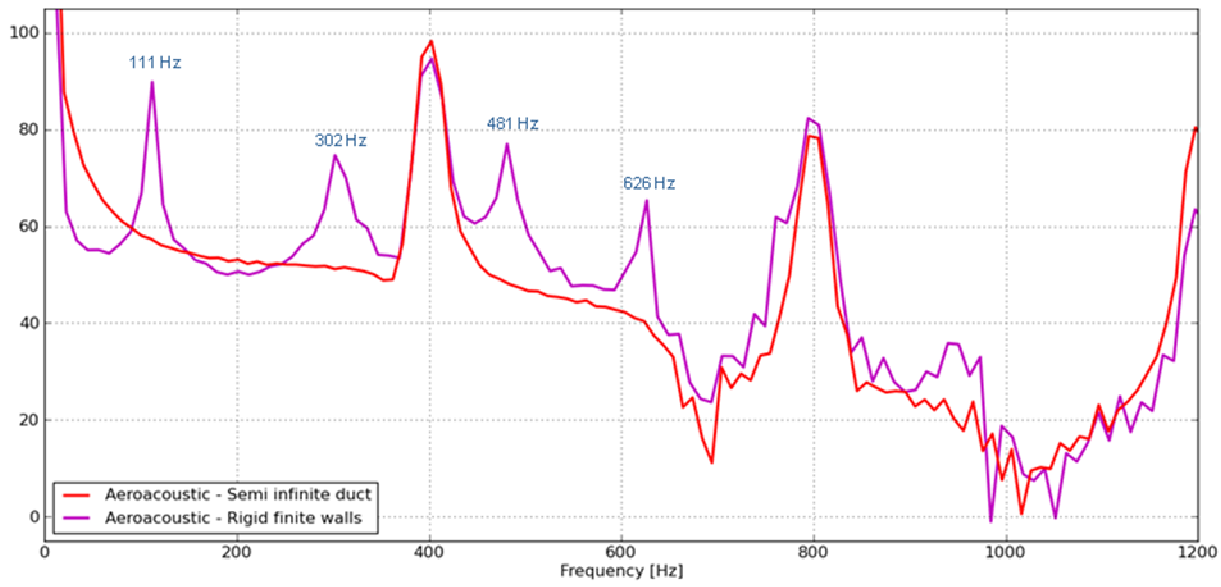

Figure 9: Sound pressure level for internal duct microphone, rigid configurations

The steel and aluminum configurations include an additional phenomenon which is the structure vibration induced by the aeroacoustic excitation. The steel configuration is comparable to the rigid configuration due to the stiffness of the structure as illustrated in Figure 10. For more flexible material as the aluminum, the sound pressure level for the internal microphone is affected by the structural dynamics of the coupled system. The acoustic duct modes resonant frequencies are shifted down with respect to the rigid walls case.

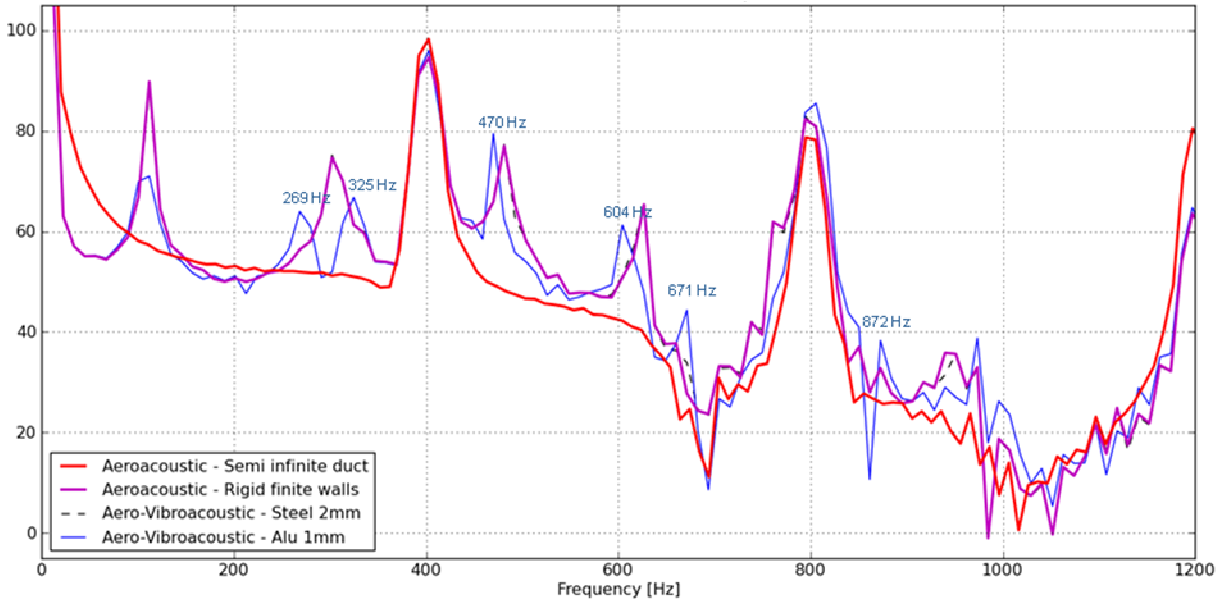

Figure 10: Comparison of the internal microphone spectra for the different configurations

The previous analysis focus on the interior noise. For the exterior noise, we use a global indicator that is the acoustic power to identify the noise transmitted at the outlet of the duct (vent) and the part transmitted by the structure. The Figure 11 shows that most of the noise radiated in the far field comes from the duct vent. Close to 270 Hz the noise transmitted through the structure is larger that the outlet (vent) contribution.

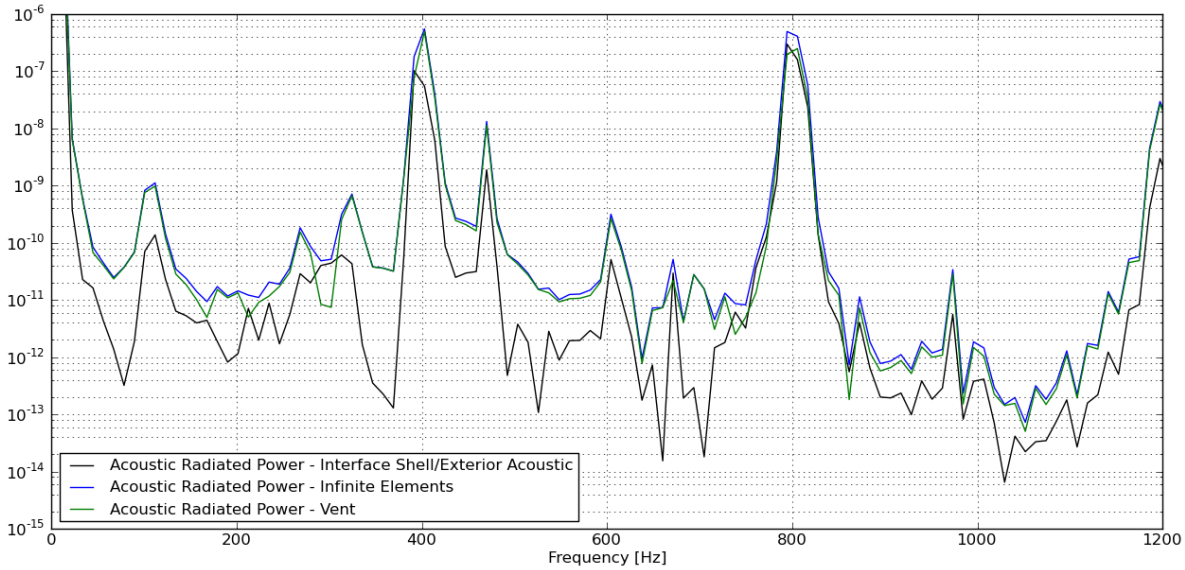

Figure 11:Comparison of the power transmitted by the structure, the duct vent and total

Different configurations using different material stiffness would lead to similar effects at different frequencies, showing the interest of a coupled aero-vibro-acoustic simulation for design of systems involving a fan..

CONCLUSIONS

This paper illustrates the computational process to simulate the fan noise using the Lighthill analogy in a finite element context. The velocity and density solution generated by a turbulent compressible CFD simulation are processed to compute equivalent noise sources according to the Lighthill's equation. The propagation of these aeroacoustic sources is then computed thanks to the acoustic solver and the blade passing frequencies and its harmonics are clearly visible on the virtual microphone located inside the acoustic fluid. The surface contribution located at the interface between static and rotating part represent the main noise sources. This part supports the acoustic noise sources from the rotating part: in other words, the noise sources located around the blades represent the main noise sources. A special care in CFD mesh generation on the interface ensures that the surface contribution is not affected by spurious numerical fluctuations. The volume sources are responsible for the broadband noise between blade passing frequencies.

The aeroacoustic model can be completed by vibro-acoustic features in order to take into account the effects of the flexible structure. This model corresponds to classical casing properties. In a further step, some acoustic treatments (such as foam) could be included to reduce the noise transmission.

BIBLIOGRAPHY

[1] A. Guédel – *Bruits des ventilateurs,* Techniques de l'ingénieur, traité de Génie mécanique, **1999**

[2] S. Caro, R. Sandboge, R. Ambs, K. Washburn – *Validation of a CAA formulation based on Lighthill's analogy using AcuSolve and Actran/LA on a idealized automotive HVAC blower and on an axial fan,* AIAA 2006-2692, **2006**

[3] S. Caro, Y. Nishio, R. Sandboge, J. Iyer – *Presentation of a CAA formulation based on Lighthill's analogy for fan noise,* Proceedings of Fan Noise 2007 Symposium, Lyon, **2007**

[4] S. Caro, P. Ploumhans, X. Gallez – *Implementation of Lighthill's Acoustic Analogy in a Finite/Infinite Elements Framework,* AIAA Paper 2004-2891, 10th AIAA/CEAS Aeroacoustics Conference and Exhibit, Manchester, UK., **2004**

[5] M.-J. Lighthill – *On Sound Generated Aerodynamically*, Proc. Roy. Soc., London, Vol. A 211, **1952**

[6] A. Oberai, F. Ronaldkin, T. Hughes – *Computational Procedures for Determining Structural-Acoustic Response due to Hydrodynamic Sources*, Comput. Methods Appl. Mech. Engrg., Vol. 190, pp. 345-361 **2000**

[7] A. Oberai, F. Ronaldkin, T. Hughes – *Computation of Trailing-Edge Noise due to Turbulent Flow over an Airfoil*, AIAA Journal, Vol. 40, pp. 2206-2216 **2002**

[8] S. Caro, Y. Detandt, J. Manera, R. Toppinga, F. Mendonça – *Validation of a New Hybrid CAA strategy and Application to the Noise Generated by a Flap in a Simplified HVAC Duct,* AIAA paper 2009-3352, 15th AIAA/CEAS Aeroacoustics Conference , Miami, Florida, **2009**